A New AC/AC Multilevel Converter Family

Martin Glinka, *Member, IEEE,* and Rainer Marquardt

***Abstract*—A new ac/ac modular multilevel converter (M^2LC) family will be introduced. The new concept stands out due to its modularity and superior control characteristics.**

The stringent modularity results in a very cost-efficient and versatile converter construction. This new M^2LC concept is well suited to a wide range of multiphase ac/ac converters. The basic working principle together with the static and dynamic behavior are explained in detail on a single-phase ac/ac converter enabling four-quadrant operation.

It is demonstrated that this converter concept fulfils the demanding requirements for future ac-fed traction vehicles very well.

***Index Terms*—Emerging topologies, matrix converters, multilevel converters, power transmission, traction.**

I. INTRODUCTION

SUPPORTED by the fast development of high-power semiconductors over recent years, multilevel converters have emerged and enable better line-side behavior than current converter topologies [6]. They also facilitate new fields of applications [2]–[11]. The presented line-side-switched modular multilevel converter (M^2LC), applied to ac-fed traction vehicles, enables additional advantages. In this application, the elimination of the bulky line transformer, increased efficiency, as well as a significantly improved transient behavior of the converter system is achieved.

The core of this new converter concept (Fig. 1) is a single-phase ac/ac M^2LC; operating directly on the 15-kV/16.7-Hz power line, it feeds directly a compact medium-frequency (MF) transformer. This concept facilitates four-quadrant operation and extremely good line-side behavior under steady-state and transient conditions. Passive *LC* filters on the line side or resonant tank circuits tuned to the double line frequency are eliminated.

This single-phase ac/ac M^2LC can be extended in order to form a one-phase/three-phase ac/ac M^2LC (Fig. 4) or any other type of multiphase converter. Their characteristics are similar to the ones of the described single-phase converter. Therefore, this paper concentrates on the single-phase converter in order to introduce the basic characteristics of the converter family.

Manuscript received November 26, 2003; revised January 16, 2004. Abstract published on the Internet March 14, 2005. This work was supported by Siemens Transportation Systems. An earlier version of this paper was presented at the 5th IEEE International Conference on Power Electronics and Drive Systems, Singapore, November 17–20, 2003.

M. Glinka was with the Institute of Power Electronics and Control, Universität der Bundeswehr München, 85579 Munich, Germany. He is now with Siemens Transportation Systems, 91052 Erlangen, Germany (e-mail: Martin.Glinka@siemens.com).

R. Marquardt is with the Institute of Power Electronics and Control, Universität der Bundeswehr München, 85579 Munich, Germany (e-mail: Rainer.Marquardt@unibw-muenchen.de).

Digital Object Identifier 10.1109/TIE.2005.843973

Besides this ac/ac M^2LC concept, other dc/ac M^2LC converters have already been presented [1], [4].

II. STRUCTURE OF THE NEW CONVERTER CONCEPT

The new single-phase M^2LC operates directly on the ac power line. It connects an MF transformer to the power line (Fig. 1). The structure of this new converter will be discussed in the following section. The voltage v_{tr} of about 13.5-kV amplitude is transformed by the MF transformer to about 2.7 kV, which can be handled by full-bridge inverters using conventional insulated gate bipolar transistors (IGBTs). The frequency of the transformer voltage is typically in the range of a few kilohertz. Here, the operation with a 1-kHz transformer will be shown.

An additional advantage of this new traction converter concept (Fig. 1) is the elimination of passive resonant tank circuits tuned to the second harmonic of the power line voltage. This is due to the fact that the M^2LC is able to compensate the severe power pulsation of the power line directly. Neglecting the power pulsation with the double transformer frequency, the M^2LC transmits practically constant power.

The transmission of constant power via the transformer—as well as the fact that only one concentrated MF transformer is needed—results in a very cost-efficient design with a high efficiency and a good power-to-weight ratio. These characteristics can also be achieved because of a good power-to-insulation-voltage ratio as well as the low demands concerning the transformer stray inductance.

III. NEW SINGLE-PHASE AC/AC-M^2LC

The M^2LC converts the power line voltage v_{line} of 15 kVrms and 16.7 Hz into the MF voltage v_{tr} and it also absorbs the second harmonic of the power line, as mentioned above. Between the power line and the M^2LC only a very small line choke L_{line} (Fig. 1) is necessary. This results from the high-quality converter voltage $v_{\mathrm{M^2LC}}$ being a pulsewidth-modulated multilevel voltage with adjustable fine voltage steps.

A. Structure of the M^2LC

The single-phase M^2LC consists of four identical multilevel converter arms (Figs. 2 and 3). Each converter arm consists of N identical submodules. The submodules (Fig. 3) contain full bridges and associated dc storage capacitors. Full four-quadrant operation of the converter is achieved without any additional connections or energy transfer to the dc storage capacitors of the submodules. In a first step, the arms may be considered as controlled voltage sources.

All submodules have the same semiconductor ratings as well as the same capacitance. For this reason all submodules are

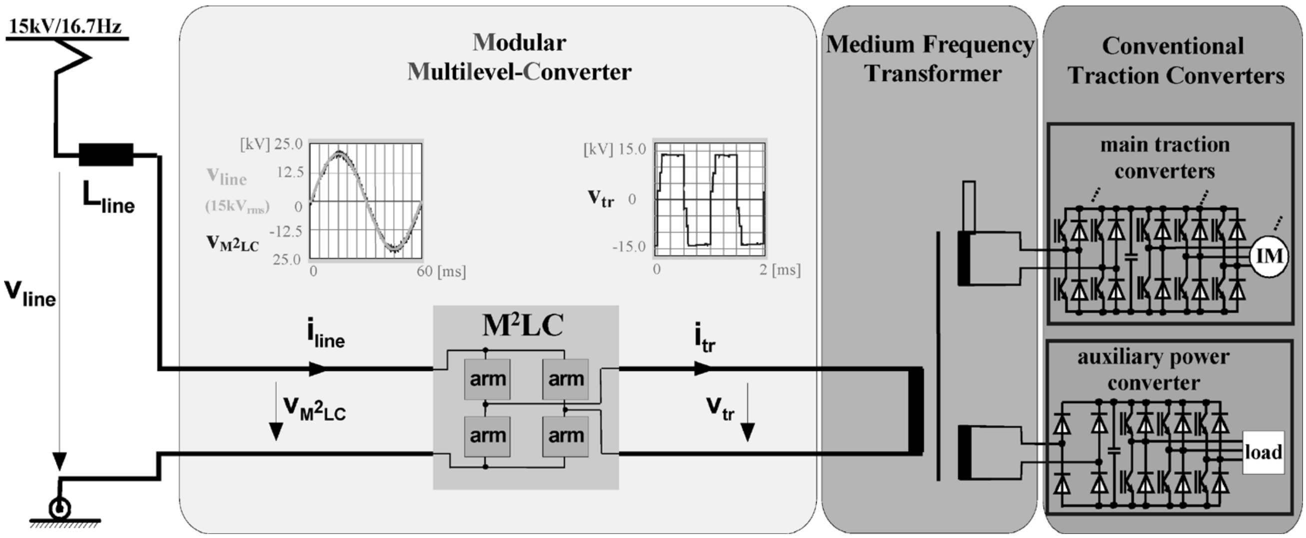

Fig. 1. Traction converter concept for the operation on the 15-kV/16.7-Hz power line.

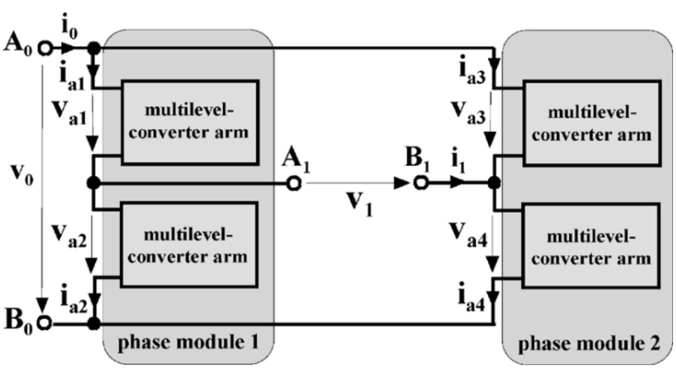

Fig. 2. AC/AC single-phase M^2LC topology.

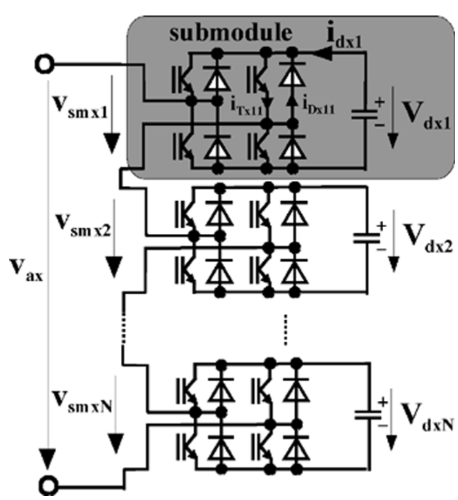

Fig. 3. Scheme of a multilevel converter arm.

identical two-terminal devices. The power supply for the IGBT drivers of each submodule is taken out of the associated capacitors. Therefore, the submodule has (next to these two terminals) only one interface. It is a duplex fiber-optic interface which connects the submodule to the central control unit. This unit controls the whole operation of the M^2LC.

The converter basically consists of $4N$ identical submodules (Fig. 3). This is not only a strong advantage concerning maintenance aspects; it also features a very consistent redundancy concept. Even though different submodules might have different tasks during the operation, they can easily be replaced by each other.

Two further advantages are worth mentioning in comparison to other multilevel inverters (like the diode-clamped inverter as well as the capacitor-clamped inverter [6]). First of all, the stringent modular topology of the M^2LC enables a very versatile converter, which can be easily adapted to different voltage and power levels. The other additional advantage is the fact that no high-voltage dc link is needed to interconnect all submodules of the M^2LC with low inductive busbars. Therefore, all submodules and arms can be connected to each other with ordinary cables.

It can be assured with a central and redundant converter control that a failure of any submodule will not cause any secondary fault in other components of the converter. This is realized by observing all converter arm currents with the central control.

In case of any failure at least two arm currents will exceed their limits. The central control receives this information via an optical interface within a few microseconds [5] and switches off all IGBTs of the whole converter within about the same time period.

Therefore, any semiconductor, IGBT driver, or duplex fiber-optic cable failure can solely deactivate the corresponding submodule. This feature also assures that the converter is short-circuit proof with respect to all output terminals. It can be assured that the terminals of the faulty submodule are short circuited. Therefore, the corresponding arm can still operate with one voltage level less, but no further restrictions.

This combination of the identical two-terminal submodules together with their simple and robust interconnections results in a converter structure that enables high availability.

The central control unit of the converter communicates with all submodules and the current transducers via duplex fiber-optic interfaces. Such a control unit is realized as part of a M^2LC

prototype converter [5]. The way the voltages of all storage capacitors can be controlled will be explained further on.

B. Basic Operation

With the single-phase M^2LC two bipolar voltages v_0 and v_1 can be impressed, fully independent from each other (Fig. 2). Concerning the traction converter, the voltages v_0 and v_1 of the M^2LC (Fig. 2) correspond to $v_{\mathrm{M^2LC}}$ and v_{tr} (Fig. 1). Since the topology of the M^2LC is absolutely symmetric, it does not make any difference if v_0 corresponds to $v_{\mathrm{M^2LC}}$ and v_1 to v_{tr} or vice versa.

The M^2LC can impress both voltages v_0 and v_1 fully independent from each other by an appropriate control scheme. The following equations describe the relationship between the voltages v_{ax} of the arms and the terminal voltages v_0 and v_1:

$$v_{a1} = v_{a4} = \frac{v_0 - v_1}{2} \tag{1}$$

$$v_{a2} = v_{a3} = \frac{v_0 + v_1}{2} \tag{2}$$

$$\hat{v}_{ax} \geq \frac{\hat{v}_0 + \hat{v}_1}{2}. \tag{3}$$

The basic working principle of the converter is explained in the following by regarding all converter arms as analog voltage sources. This assumption is valid because each arm voltage is impressed with pulsewidth modulation (PWM). Several different PWM methods can be chosen for this task.

When each desired arm voltage $v_{a1} \ldots v_{a4}$ is impressed as defined by (1) and (2), the desired voltages v_0 and v_1 are consequently impressed on the output terminals.

In order to be able to impress two completely independent voltages v_0 and v_1 with different frequencies and amplitudes, each arm has to always be able to impress the voltage amplitude $\hat{v}_{ax}$. Equation (3) describes the relationship between the required minimum voltage amplitude $\hat{v}_{ax}$ of each arm and the maximum amplitudes of the output voltages v_0 and v_1.

The minimum number of submodules ($N_{\mathrm{SM\_p\_arm}}$) needed per arm is described by

$$N_{\mathrm{SM\_p\_arm}} \geq \frac{\hat{v}_{ax}}{V_{d\,\mathrm{min\_\,av}}} \tag{4}$$

where $V_{d\,\mathrm{min\_\,av}}$ is the average minimum voltage of all submodule voltages V_{day} of the corresponding converter arm.

The relationship between the two multilevel output voltages of the converter as well as the necessary number of submodules ($N_{\mathrm{SM\_p\_arm}}$) for each arm can also be described by the following equation:

$$N_{\mathrm{SM\_p\_arm}} \geq \frac{(m_0 - 1) + (m_1 - 1)}{2} \tag{5}$$

with an m_0-level bipolar voltage v_0 and an m_1-level bipolar voltage v_1.

Based on the assumption that all storage capacitor voltages of the whole converter are equal, the following instantaneous current distribution (7) and (8) will be impressed when the arm voltages are impressed as defined by (1) and (2). In this case, the terminal current i_0 is split up between the two phase modules 1 and 2, equally, due to the fact that they impress the same voltage v_0 as described by (6) and both phase modules have the same impedance with respect to the terminal voltage v_0. Equation (6) can be derived directly from (1) and (2).

Due to the fact that the converter is symmetrical, the terminal current i_1 will also split up symmetrically between the corresponding phase modules. Therefore, the instantaneous arm currents of (7) and (8) will be impressed

$$v_{a1} + v_{a2} = v_{a3} + v_{a4} = v_0 \tag{6}$$

$$i_{a1} = i_{a4} = \frac{i_0}{2} + \frac{i_1}{2} \tag{7}$$

$$i_{a2} = i_{a3} = \frac{i_0}{2} - \frac{i_1}{2}. \tag{8}$$

C. Control of the DC Storage Capacitor Voltages

In the above section it was described how the converter—based on the assumption that all the submodules can be regarded as ideal two-level bipolar voltage sources—can impress the output voltages. In the following, it is described how the dc storage capacitors of the submodules can be controlled in practice so that they can be used as reliable voltage sources.

By impressing v_0 and v_1, the equivalent input and output currents can be controlled. Consequently, the input and output power of the converter can be controlled in this way. Nevertheless, two more tasks have to be fulfilled in order to control all dc storage capacitor voltages.

1) The stored energy within the whole converter shall be kept at a certain set-point value: this is equivalent to an identical set-point value for all submodule storage capacitor voltages.
2) The voltage levels of all dc storage capacitors have to be balanced within a reasonably tight tolerance band.

The first task is relatively simple. By monitoring all storage capacitor voltages in the central control unit, the overall stored energy can easily be derived. By adapting the input and output power of the converter, the overall stored energy can be adjusted to its set-point value. Instead of using the stored energy as a control parameter, the average voltage of all storage capacitors can also be used as an equivalent parameter. This parameter can easily be calculated from the monitored capacitor voltages. For small variations around this average voltage, a negligible error will be made.

In the case where the first task is fulfilled and all storage capacitors are balanced as well, the capacitor voltages have reached their set-point value. To keep all storage capacitors balanced the following method can be used.

- All four converter arms have to be controlled in such a way that the stored energy in all arms is about equal.
- The voltage balancing within one converter arm can be realized in the following way.
  – When the converter arm will absorb power the submodules with the lowest storage capacitor voltages will be used in order to impress the desired arm voltage.
  – When the converter arm will supply power it is vice versa and the submodules with the highest storage capacitor voltages will be used in order to impress the desired arm voltage.

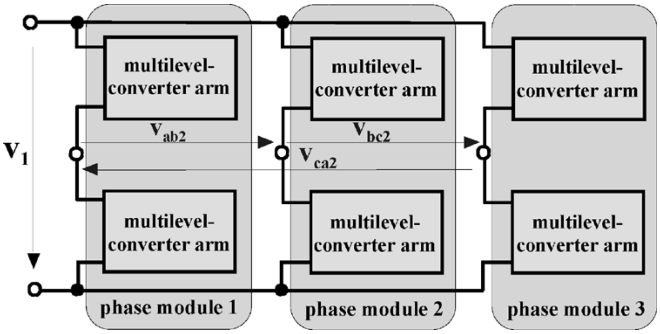

Fig. 4. One-phase/three-phase ac/ac M^{2}LC topology.

IV. Other Multiphase AC/AC M^{2}LCs

The modular-multilevel converter topology of the single-phase converter can be extended to a one-phase/three-phase M^{2}LC (Fig. 4). As one can see, just one extra phase module has to be added in order to develop this converter from the single-phase M^{2}LC. The static and dynamic performance of this new converter topology is similar to the one of the single-phase M^{2}LC. Besides this multiphase M^{2}LC, a three-phase/three-phase M^{2}LC topology, whose structure is comparable to matrix converters, is possible. In analogy, any other multiphase M^{2}LC can be realized.

The number of arms ($N_{\rm arm}$) of any multiphase M^{2}LC is described by the following equations:

$$n_{\mathrm{ph}x} = \begin{cases} 2, & m_{\mathrm{ph}x} = 1 \\ m_{\mathrm{ph}x}, & m_{\mathrm{ph}x} \geq 3 \end{cases} \tag{9a}$$

$$N_{\mathrm{arm}} = n_{\mathrm{ph0}} * n_{\mathrm{ph1}} \tag{9b}$$

where $m_{\rm ph0}$ is the number of phases of the primary voltage system and $m_{\rm ph1}$ is the number of phases of the secondary voltage system. Therefore, a one-phase/three-phase M^{2}LC with $n_{\rm ph0} = 2$ and $n_{\rm ph1} = 3$ has six arms (Fig. 4) and a three-phase/three-phase M^{2}LC with $n_{\rm ph0} = 3$ and $n_{\rm ph1} = 3$ has nine arms, for example. In such a three-phase/three-phase matrix converter each phase of the primary voltage system will be connected to all other phases of the secondary voltage system via one converter arm of the M^{2}LC. Equations (4) and (5) can also be used for multiphase M^{2}LCs in order to derive the necessary number of submodules per arm.

V. Expenditure of Installed Components

A. Capacitive Energy Storage Requirements

Looking at the performance of the single-phase M^{2}LC, one has to keep in mind that it must transmit line-side power that pulsates with the second harmonic of the line voltage. However, the transmitted power on the transformer side is practically constant. Therefore, the power pulsation has to be absorbed by the converter itself. This results in a pulsating dc voltage $v_{\rm dav}$ of the local storage capacitors (Fig. 6), which can be allowed for the new converter concept. Without restrictions, a high-voltage ripple around the nominal value of Δv_d (±20%) can be realized.

For the investigated design of a 5-MW converter, the submodules are realized with 3.3-kV IGBTs and 940-μF/1900-V storage capacitors. Each converter arm consists of $N = 12$ submodules. This includes one submodule per phase for redundant operation.

For this voltage range of the converter with a maximum voltage amplitude of $\hat{v}_{\rm M^2LC} > 27$ kV on the 15-kV/16 2/3-Hz power line, other IGBT blocking voltages could well be the optimal choice, depending on several aspects. The modularity of the M^{2}LC gives the freedom to choose from a wide range of switches.

Due to the high-voltage ripple of the storage capacitors, the energy storage requirements can be limited to a level equal to or less than needed for conventional systems.

The nominal stored energy of the 5-MW M^{2}LC is 83 kJ in total. The stored energy in the related traction converters can be reduced considerably when they are fed from a M^{2}LC. This results in an energy storage requirement of about 18 kJ per 1-MW nominal converter power in total. For conventional state-of-the art traction converters (e.g., 6.5-MW locomotive 152 of the German Railway) that operate on the 15-kV/16.7-Hz power line, the nominal stored energy in the related dc capacitors as well as the resonant tank circuits is also in this range or even slightly above it. Therefore, the new converter concept has equal energy storage requirements compared to state-of-the-art systems and does not suffer from excessive energy storage requirements.

B. Semiconductor Requirements

In order to minimize the converter losses together with the installed silicon area, the following goals will have to be reached:

- effective exploitation of the semiconductor blocking voltage;
- symmetric current distribution in all valves over all operation points (power factor, sign of energy transmission);
- minimal switching frequencies of the IGBTs.

The conduction losses of converters can be minimized with an effective exploitation of the semiconductor blocking voltage and a symmetric current distribution in the semiconductors.

For the reason that the voltages across the semiconductors of each submodule are well clamped by their corresponding local storage capacitor, a good exploitation of the semiconductor blocking voltage can be assured.

With respect to symmetric current distribution, it will be shown that the average current of all semiconductor valves of the M^{2}LC is equal. It will also be demonstrated that this current distribution is independent of the operation point of the converter. This independent current distribution is kept for any power factor and direction of power transmission.

The required total silicon area can be assumed to be proportional to the total semiconductor power losses, if the cooling system is the limiting factor. This assumption is reasonable for high-power converters. Therefore, a symmetric current distribution on all semiconductor valves results in an optimal exploitation of the installed silicon area.

The relationship between the average of the absolute values of the output load currents i_0, i_1, and the arm current i_{ax} is

$$\overline{|i_{ax}|} = \max\left(\frac{\overline{|i_0|}}{2}, \frac{\overline{|i_1|}}{2}\right). \tag{10}$$

This is due to the fact that the converter can be controlled without any restrictions in such a way that each load current will always be equally split up between both corresponding phase modules (Fig. 2).

All submodules of one arm have to conduct the same arm current i_{ax}. It will now be shown that this arm current is equally split up between all semiconductors of each submodule.

For every pair of semiconductor switch and antiparallel diode (11) can be derived using Kirchhoff's first law. The orientation of the storage capacitor current i_{dxy} is shown in Fig. 3.

$$\overline{i_{Txyz}} = \overline{i_{Dxyz}} + \frac{\overline{i_{dxy}}}{2}. \tag{11}$$

The only precondition for this equation is the fact that the storage capacitor current has to be equally split up between both phases of the submodule's full-bridge inverter. This can be easily fulfilled by an appropriate control.

As long as both converter output voltages v_0 and v_1 have no dc component, the arm voltages will also not have any dc component. In this case, the following equation can be derived using Kirchhoff's first law:

$$\frac{\overline{|i_{ax}|}}{2} = \overline{i_{Dxyz}} + \overline{i_{Txyz}}. \tag{12}$$

With (8) and (12), (13) and (14) can be derived

$$\overline{i_{Txy1\ldots4}} = \frac{1}{4}\overline{|i_{ax}|} + \frac{1}{4}\overline{i_{dxy}} \tag{13}$$

$$\overline{i_{Dxy1\ldots4}} = \frac{1}{4}\overline{|i_{ax}|} - \frac{1}{4}\overline{i_{dxy}}. \tag{14}$$

Each submodule absorbs practically no real power, therefore, the average value of the storage capacitor current i_{dxy} is practically zero in steady state. This condition is fulfilled independently of the power factor of the converter as well as the sign of the power transmission. Therefore, the following equation results:

$$\overline{i_{Txy1\ldots4}} = \overline{i_{Dxy1\ldots4}} = \frac{1}{4}\overline{|i_{ax}|}. \tag{15}$$

In consequence, the average current in all converter semiconductors is 1/8 of the maximum of the absolute value's average of both terminal currents i_0 and i_1 [(10) and (15)]. The average values of the semiconductor currents are symmetrically distributed and independent of the operation point of the converter (power factor and sign of power transmission).

This result also indicates that an optimal converter efficiency can be achieved if both terminal currents have similar amplitudes (Fig. 5).

With respect to the necessary IGBT switching frequency, it can be shown that it is significantly lower than the resulting PWM frequency at the terminals.

With a 4-kHz PWM-modulated voltage on the line side and a 1-kHz block voltage on the transformer side, the resulting average switching frequency of all 3.3-kV-IGBTs is about 300 Hz.

This low IGBT switching frequency contributes to the good efficiency of the M^2LC (Fig. 5). In generalized form, the following components contribute to the average IGBT switching frequency expressed by:

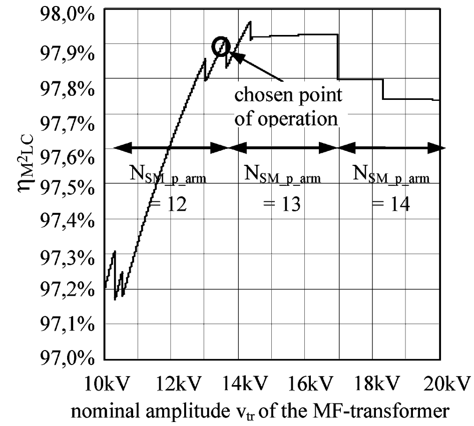

Fig. 5. Efficiency $\eta_{\mathrm{M^2LC}}$ of single-phase ac/ac M^2LC with $f_{\mathrm{tr}} = 1$ kHz, $V_{\mathrm{line}} = 15\ \mathrm{kV_{rms}}$, and $f_{\mathrm{pwm\_line}} = 4$ kHz at nominal power of 5 MW.

$$f_{\mathrm{SM}} = f_{\mathrm{SM}_{V0}} + f_{\mathrm{SM}_{V1}} + f_{\mathrm{SMpwm}_{V0}} + f_{\mathrm{SMpwm}_{V1}} + f_{\mathrm{SMsymm}}. \tag{16}$$

The output voltage amplitudes $\hat{v}_x$ as well as the average minimum storage capacitor voltage $V_{d\,\mathrm{min\_av}}$ influence the component $f_{\mathrm{SM}vx}$ at the moment when both voltage amplitudes $\hat{v}_x$ have to be realized. The value of N_{Vx} describes how many voltage steps add up to the output voltage amplitude

$$N_{Vx} = \mathrm{ceil}\left(\frac{\hat{V}_x}{V_{d\,\mathrm{min\_av}}}\right). \tag{17}$$

Together with this information, the number of submodules per arm $N_{\mathrm{SM\_p\_arm}}$ (4) as well as the fundamental frequency f_{vx} of the terminal voltages, $f_{\mathrm{SM}_{Vx}}$ can be derived

$$f_{\mathrm{SM}_{Vx}} = f_{Vx}\mathrm{ceil}\left(\frac{N_{Vx}}{2N_{\mathrm{SM\_p\_arm}}}\right). \tag{18}$$

Therefore, $f_{\mathrm{SM}vx}$ is the average switching frequency component of each submodule that is caused by the frequency of the corresponding terminal voltage frequency f_{Vx}.

The realization of the PWM voltage signals can be split up equally among all submodules of one phase module. Therefore, the average submodule frequency which depends on the corresponding output PWM frequencies is

$$f_{\mathrm{SMpwm}_{Vx}} = \frac{f_{\mathrm{pwm}_{Vx}}}{2N_{\mathrm{SM\_p\_arm}}}. \tag{19}$$

In order to receive the average submodule frequency f_{SM} with (16), there is only the component f_{SMsymm} missing. This component describes how often the submodule has to be switched on average in order to improve the active voltage balancing within each converter arm. No general rule can be given for this component. In applications with higher pulse frequencies no additional switching instants will be necessary, therefore, $f_{\mathrm{SMsymm}} = 0$.

For the present application, $f_{\mathrm{SMsymm}} = 85$ Hz proved to be sufficient. Therefore, the active voltage balancing within each arm increases the overall switching frequency by less than 15%.

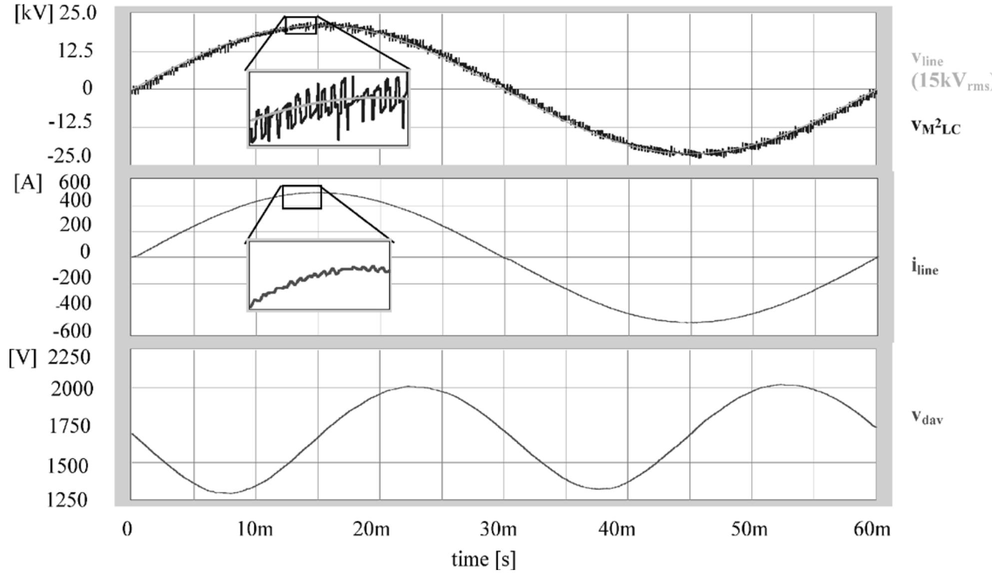

Fig. 6. Simulation results of the operation at nominal power of 5 MW on the 15-kV/16.7-Hz power line.

The average switching frequency of each IGBT in a submodule is given finally by

$$f_{\mathrm{IGBT}} = \frac{f_{\mathrm{SM}}}{2}. \tag{20}$$

Besides the single-phase ac/ac M^{2}LC, (11)–(15) and (17)–(20) are also valid for multiphase ac/ac M^{2}LCs, and only (10), (16), and (20) have to be adapted slightly in order to take into account that further output terminal voltages do exist.

C. Gate Driver Circuits and Their Power Supplies

Neutral-point-clamped (NPC) inverters [6], realized in a back-to-back configuration, would be one of the most common alternatives to the ac/ac M^{2}LC. Compared to a back-to-back NPC converter, the AC/AC-M^{2}LC needs twice as many driver circuits for a single-phase converter.

The higher number of gate drivers would result in lower reliability as well as slightly higher costs. Several measures have been taken in order to compensate for this drawback of the M^{2}LC family.

The measures that have been taken are presented in [5]. The following short list contains the developed countermeasures:

- one duplex fiber-optical interface for the transmission of 4 IGBT switching signals as well as voltage and error signals;
- local power supplies without high-voltage insulation operating from the local storage capacitor;
- minimization of the number of interfaces per submodule to two output terminals for cable connections plus one duplex fiber-optical interface.

D. Converter Efficiency

Fig. 5 shows the converter efficiency as a function of a varying voltage amplitude of the MF transformer. It can be seen that a very good efficiency of nearly 98% at nominal power can be achieved, combined with relatively high PWM frequencies.

The efficiency at partial load is even better—at least down to approximately 15% of nominal power.

The presented efficiency calculation is based on the following conditions.

- Conduction losses as well as switching losses are calculated on the data basis of the 3.3-kV/1.2-kA IGBT module from Mitsubishi (CM1200HC-66H—third generation); the silicon area of the IGBTs as well as the diodes has been downscaled by a factor of 4 to a nominal current of 300 A.
- The switching loss calculation is based on the assumption that the switching losses in the IGBTs are proportional to the switched current as well as the corresponding storage capacitor voltage V_{dx}.
- The diode switching losses have been neglected

VI. Operation Characteristics of the Converter

This section presents the steady state as well as the transient operation characteristics of the converter. For this purpose, detailed simulation results of a 5-MW converter will be used.

A. Operation on the 15-kV/16 2/3-Hz Power Line

In this section, the basic operation characteristics of the converter topology are presented. This is done in detail for the 15-kV/16.7-Hz power line. The new system is well suited for multisystem operation with different voltages and frequencies. It is shown in [2] that the converter can be operated at two different power lines, 15-kV/16.7-Hz and 25-kV/50-Hz with little extra expenditure and no additional mechanical switches.

In Fig. 6, the line current i_{line} as well as the line voltage and the associated converter input voltage $v_{\mathrm{M^2LC}}$ are shown for a steady-state operation point of 5-MW nominal power. It can be seen that the converter impresses an extremely smooth line current. Line voltage and line current are in phase with each other ($\cos\varphi = 1$).

In order to be able to transfer a constant power of 5 MW via the MF transformer, the M^{2}LC has to store a considerable

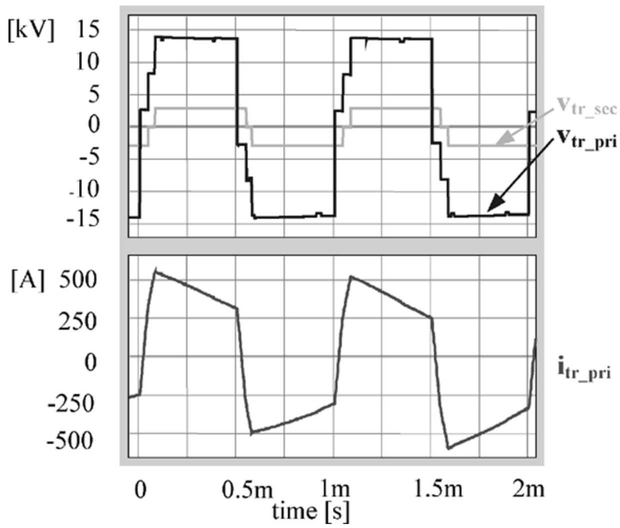

Fig. 7. Simulation results of the transformer operation at nominal power of 5 MW.

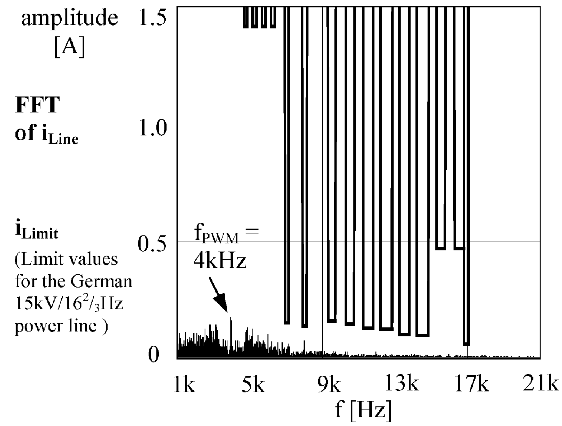

Fig. 8. Harmonics of the line current at 5 MW and 15-kV/16.7-Hz line voltage.

amount of energy. This requirement is caused by the unavoidable power pulsation of the single-phase line side. The energy can be equally stored in all dc storage capacitors of the M^{2}LC. This energy storage results in the pulsation of the voltage average v_{dav} of all dc storage capacitors (Fig. 6).

Although v_{dav} pulsates with up to $+/-20\%$ around its nominal value, there is no noticeable impact on the line current or the transformer currents (Figs. 6 and 7). This behavior is achieved because the control can adapt the pulse control factor of the related submodules for each PWM period.

The current and voltage waveforms of the 1-kHz transformer are shown in Fig. 7. The transformer has a turns ratio of 5 : 1. By adjusting the phase shift between primary and secondary side, the transferred power can be changed easily and very quickly. The transformer ratio has primarily been chosen to realize an optimum with respect to the M^{2}LC efficiency as well as semiconductor costs.

By choosing an optimized transformer ratio, the required total silicon area can be kept at a level equal to or less than that required for comparable 5-MW high-voltage multilevel converters. In the presented simulations all full-bridge inverters, which would be connected to the secondary side of the MF transformer, are combined in a single two-level full-bridge inverter of full power rating.

In Fig. 8, the line current harmonics are presented. They have been calculated with a fast Fourier transform (FFT) of the line current i_{line} (Fig. 6). This graph also contains the current limits of the German 15-kV/16.7-Hz power line over the relevant spectrum.

It can be seen that the converter spectrum fulfills well this very demanding task. The 4-kHz PWM frequency on the line side can also be seen clearly (Fig. 8).

B. Operation Under Harsh Transient Conditions on the 15-kV/16.7-Hz Power Line

The simulation results shown in Fig. 9 demonstrate the very good dynamic behavior of the M^{2}LC under extreme operation conditions. A sudden interruption of the bow contact of the traction vehicle is assumed. These frequent interruptions typically take place for less than 15 ms. The bow contact interruption occurs in the simulation at a maximum power line voltage level of 18.5 kV$_{\mathrm{rms}}$. After several hundred microseconds, the converter control recognizes the current interruption and steadily reduces the transferred power on the transformer side (P_{tr}) from the nominal value of 5 MW down to 500-kW auxiliary power level.

Despite this cut from the power line it can be seen that the dc voltages v_{dxy} of all submodules can be controlled well. This is clearly demonstrated by the waveforms of all dc storage capacitors $v_{d11} \ldots v_{d4N}$, which are shown in the third graph of Fig. 9. Although extreme transients have to be realized by the converter, all dc storage capacitor voltages are kept within a tight tolerance band.

In comparison to the M^{2}LC, conventional converters with resonant tank circuits are often unable to cope with such extreme transients. In these situations they often have to be cut from the power line using the main circuit breaker, which will be followed by a subsequent restarting procedure. This is due to the fact that the resonant tank circuits of these converters cannot be controlled or damped adequately. Due to the fact that the M^{2}LC does not need these filters, it can be controlled much better under such working conditions. As mentioned above, this superior performance can be achieved with about the same total stored energy as that needed for conventional systems.

VII. Conclusion

A new converter family has been introduced which stands out with a wide variety of useful characteristics. The very good dynamic behavior of this converter has been verified with simulation results.

Negligible harmonic distortion of the line-side current as well as high efficiency can be achieved with the new converter. In addition to the excellent electrical performance of the converter at steady state and extreme transients, its stringent modularity results in a very versatile design with an inherent redundancy, a high exploitation of the installed silicon, and good efficiency.

A prototype ac/ac M^{2}LC in the 2-MW power range with up to 17-level output voltage systems (eight submodules per arm)

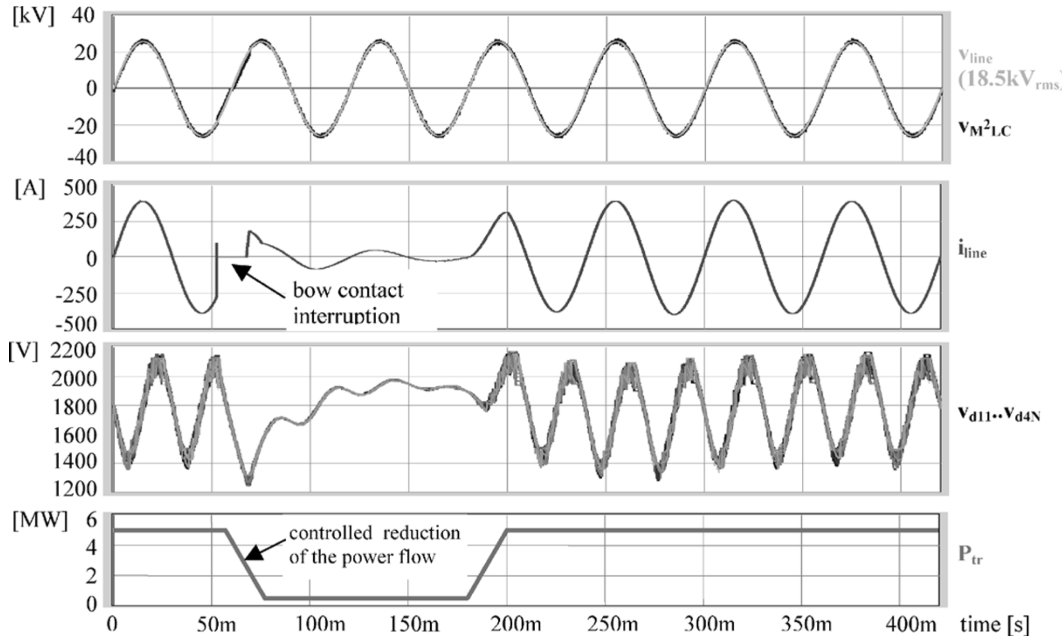

Fig. 9. Simulation of the traction converter topology at a bow contact interruption (nominal power level and maximum line voltage).

is under construction at present [5]. With this prototype converter, single-phase and multiphase M^{2}LCs and optimized control strategies can be tested under realistic operating conditions.

REFERENCES

[1] R. Marquardt and A. Lesnicar, "A new modular voltage source inverter topology," in *Proc. EPE'03*, Toulouse, France, 2003, CD-ROM.

[2] M. Glinka and R. Marquardt, "A new single-phase AC/AC-multilevel converter for traction vehicles operating on AC line voltage," in *Proc. EPE'03*, Toulouse, France, 2003, CD-ROM.

[3] ——, "A new AC/AC-multilevel converter family applied to a single-phase converter," in *Proc. PEDS'03*, Singapore, Nov. 2003, CD-ROM.

[4] A. Lesnicar, J. Hildinger, and R. Marquardt, "Modulares stromrichterkonzept für netzkupplungsanwendungen bei hohen spannungen," in *Proc. ETG-Fachbericht*, vol. 88, Bad Nauheim, Germany, Apr. 2002, pp. 155–161.

[5] M. Glinka, "Prototype of multiphase modular-multilevel-converter with 2 MW power rating and 17-level-output-voltage," in *Proc. IEEE PESC'04*, vol. 4, Aachen, Germany, Jun. 2004, pp. 2572–2576.

[6] J. Rodriguez, J.-S. Lai, and F. Z. Peng, "Multilevel inverters: A survey of topologies, controls, and applications," *IEEE Trans. Ind. Electron.*, vol. 49, no. 4, pp. 724–738, Aug. 2002.

[7] A.-C. Rufer, N. Schibli, and C. Briguet, "A direct coupled 4-quadrant multilevel converter for $16^{2/3}$ Hz traction systems," in *Proc. Int. Conf. Power Electronics and Variable Speed Drives*, London, U.K, Sep. 1996, pp. 448–453.

[8] M. Steiner, R. Deplazes, and H. Stemmler, "A new transformerless topology for AC-fed traction vehicles using multi-star induction motors," in *Proc. EPE'99*, Lausanne, Switzerland, 1999, CD-ROM.

[9] M. Steiner, "Seriegeschaltete Gleichspannungszwischenkreisumrichter in Traktionsanwendungen am Wechselspannungsfahrdraht," Ph.D. dissertation, ETH Zürich, Zürich, Switzerland, 2000.

[10] P. C. Kjaer, S. Norrga, and S. Östlund, "A primary-switched line-side converter using zero-voltage switching," *IEEE Trans. Ind. Appl.*, vol. 37, no. 6, pp. 1824–1830, Nov./Dec. 2001.

[11] S. Östlund, "A Primary Switched Converter System for Traction Applications," Ph.D., Dept. Elect. Eng., Elect. Mach., Power Electron., Royal Inst. Technol., Stockholm, Sweden, 1992.

Martin Glinka (M'00) was born in Rheinberg, Germany, in 1970. He received the Dipl.-Ing. (M.Sc.) degree in electrical engineering from the Friedrich-Alexander-Universität Erlangen-Nürnberg, Erlangen-Nürnberg, Germany, in 1997.

In November 1997, he joined Siemens A&D LD, where he developed high-power traction converters for railway applications. In December 1999, he joined the Institute of Power Electronics and Control, Universität der Bundeswehr München, Munich, Germany, as a Research Associate. In November 2004, he joined Siemens Transportation Systems, Erlangen, Germany. He is engaged in research and development of high-power multilevel converters for traction applications directly operating on the power line, as well as dc/dc converters.

Rainer Marquardt was born in Hannover, Germany, in 1953. He received the Dipl.-Ing. (M.Sc.) degree in electronic communication and the Dr.-Ing. (Ph.D.) degree in power electronics from the University of Hannover, Hannover, Germany.

He then joined Siemens AG, Erlangen, Germany, where he performed numerous industrial research and development projects for high-power applications in power transmission and advanced ac drive systems for traction applications. He has filed 48 patents in these areas. Currently, he leads the Institute of Power Electronics and Control as a Professor at the Universität der Bundeswehr München, Munich, Germany.